V.A. Barabash[1], S.A. Glyazer[1], G.G. Gromov[1], I.A. Drabkin[2], L.B. Ershova[1], S.A. Molchanova[1]

[1]RMT Ltd, 22 d, Larin Str., Nizhny Novgorod, 603152, Russia;
[2]State Scientific-Research and Design Institute of Rare-Metal Industry ("GIREDMET" JSC), 5/1 B. Tolmachevsky lane, Moscow, 119017, Russia

MATCHING OF EXTRUDED MATERIALS BASED ON BISMUTH-ANTIMONY CHALCOGENIDES FOR A THERMOELEMENT

Extruded thermoelectric materials of different conductivity types based on bismuth and antimony chalcogenides, according to the reported experimental data, are much different in their thermoelectric properties. This paper deals with matching of thermoelement legs of such materials. It is shown that condition of equality of the absolute values of Seebeck coefficient at room temperature is a good criterion for matching of materials in a thermoelement assuring maximum temperature difference on it.

Key words: extruded thermoelectric material, thermoelement, maximum temperature difference.

Introduction

Crystalline antimony-bismuth chalcogenides in their physical properties are anisotropic materials. Their characteristics in the direction of triad axis and normal to it may differ several times. In the design of thermoelements of zone-melted materials based on antimony-bismuth chalcogenides, the problem of *n*- and *p*-type legs matching does not arise, since thermoelectric characteristics of legs cut of oriented crystals in the direction normal to trigonal axis (along cleavage planes) are very close. Therefore, for matching of legs it is sufficient to take legs of different types with close electric conductivity or Seebeck coefficient values.

In extrusion of such materials, a deformation texture is formed where the major part of grains is located such that their trigonal axis is directed normal to extrusion axis. In *p*-type crystalline materials, the ratio between electric conductivity in the direction normal to trigonal axis and electric conductivity in the direction of trigonal axis (electric conductivity anisotropy) is 2 – 2.5 [1, 2], thermal conductivity anisotropy is the same as electric conductivity anisotropy; Seebeck coefficient anisotropy is absent. This results in the absence of thermoelectric figure of merit anisotropy. Therefore, in *p*-type extruded materials with ideal contacts between the grains the thermoelectric figure of merit must be the same as in a single crystal. In *n*-type materials electric conductivity anisotropy is about 4, whereas thermal conductivity anisotropy is 2. Seebeck coefficient anisotropy is absent. The difference in thermal conductivity and electric conductivity anisotropy leads to the fact that in extruded materials the lines of electric current and thermal flow may not coincide locally, which will result in formation of eddy currents [3] reduction of thermoelectric figure of merit. Therefore, in extruded materials the thermoelectric figure of merit of *n*-type materials should be lower than that of *p*-type materials, and selection of thermoelement couples becomes a topical issue.

Thermoelectric parameters of extruded materials

Temperature dependences of thermoelectric properties of extruded thermoelectric materials produced by company RMT were measured on RMT DX8080 plant. In the measurements, the six-wire

Harman method was used [4, 5]. The dimensions of the samples were (length × width × height) $2 \times 2 \times 1.6$ mm^3. Galvanic anti-diffusion *Ni* coatings were applied on the end faces of the samples by the technique used for mass production of thermoelectric modules.

The results of measurements are given in Figs. 1 – 3.

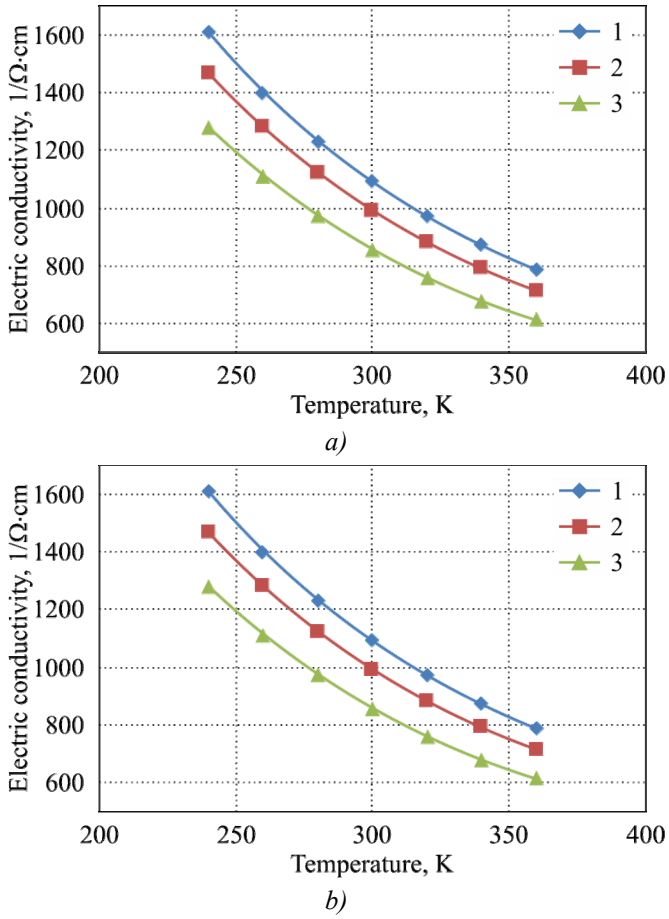

Fig. 1. Temperature dependences of electric conductivity a) for p-type $Bi_{0.4}Sb_{1.6}Te_3$ (1 – α_{300} = 200 μV/K, 2 – α_{300} = 210 μV/K, 3 – α_{300} = 216 μV/K) and b) for n-type $Bi_2Se_{0.15}Te_{2.85}$ (1 – α_{300} = –208 μV/K, 2 – α_{300} = –213 μV/K, 3 – α_{300} = –219 μV/K).

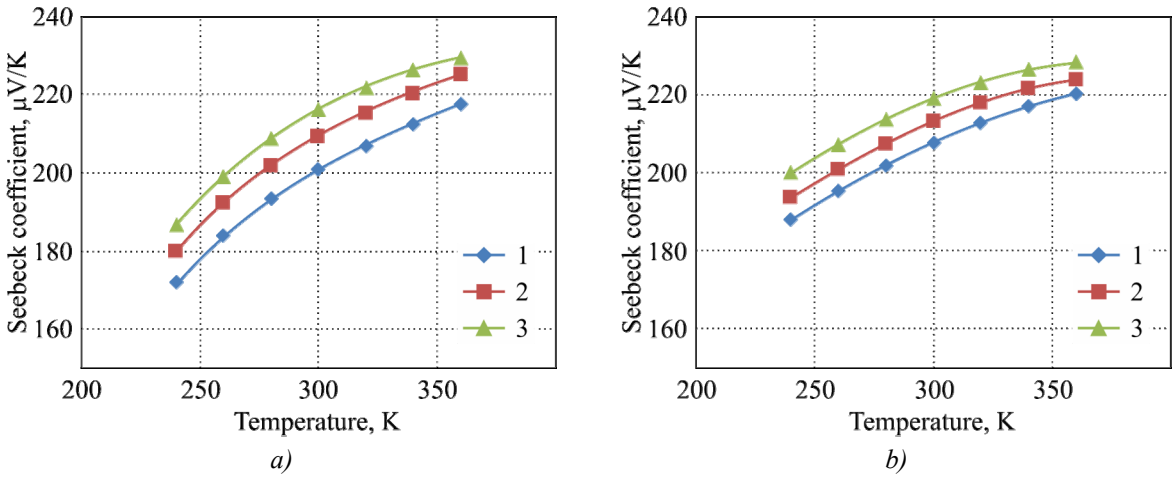

Fig. 2. Temperature dependences of Seebeck coefficient a) for p-type $Bi_{0.4}Sb_{1.6}Te_3$ and b) for n-type $Bi_2Se_{0.15}Te_{2.85}$. The designations are the same as in Fig. 1.

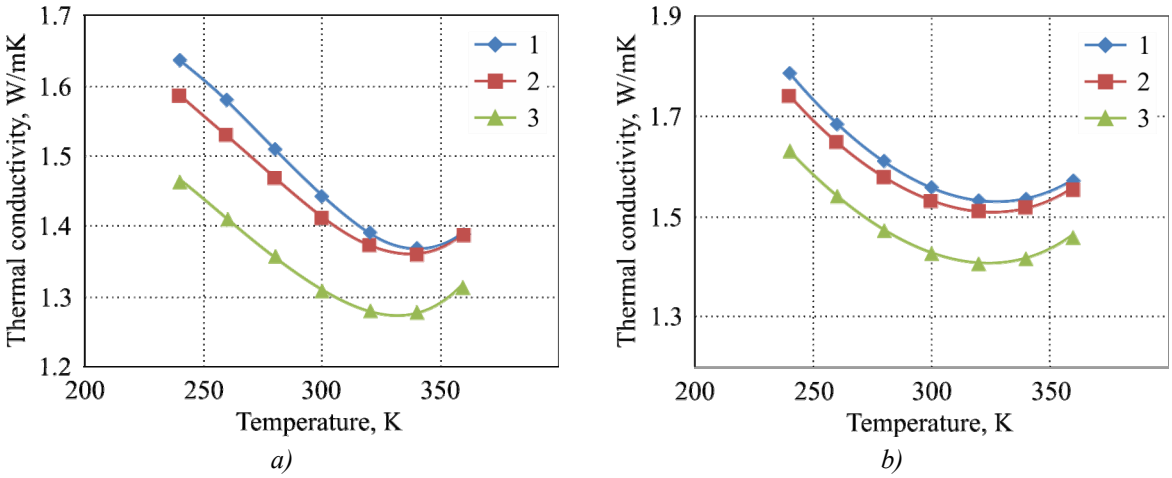

Fig. 3. Temperature dependences of thermal conductivity a) for $Bi_{0.4}Sb_{1.6}Te_3$ of p-type and b) for $Bi_2Se_{0.15}Te_{2.85}$ of n-type. The designations are the same as in Fig. 1.

The temperature dependences of the thermoelectric figure of merit are given in Fig. 4.

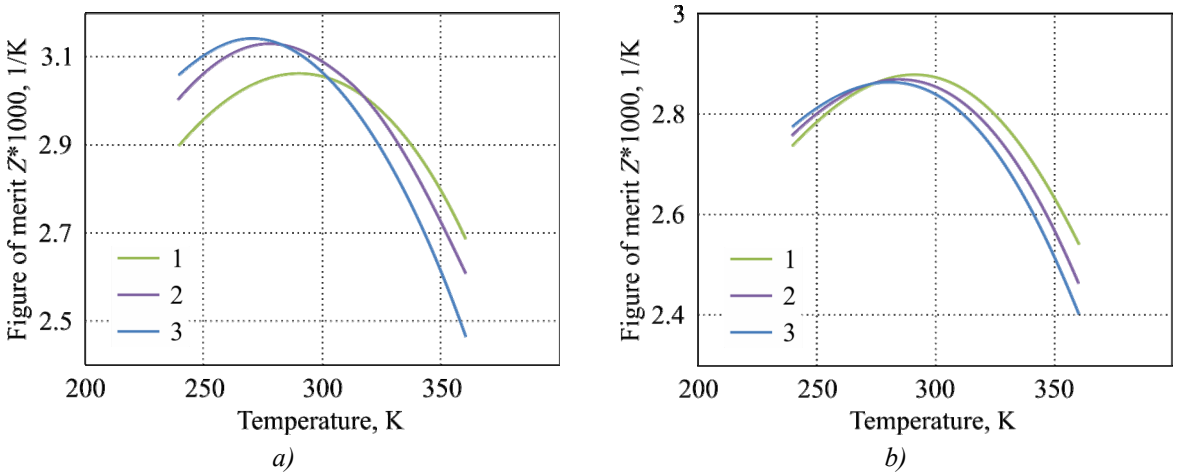

Fig. 4. Temperature dependences of thermoelectric figure of merit Z a) for p-type $Bi_{0.4}Sb_{1.6}Te_3$ and b) for n-type $Bi_2Se_{0.15}Te_{2.85}$. The designations are the same as in Fig. 1.

For the investigated samples the thermoelectric figure of merit at 300 K was $(3.05 – 3.13)\cdot10^{-3}$ K^{-1} for *p*-type and $(2.83 – 2.87)\cdot10^{-3}$ K^{-1} for *n*-type. These values are slightly below for *p*-type than published in the literature [6, 7], which may be due to a low elongation ratio (≈ 10) in extrusion tool employed. From the figure it is seen that at 300 K in *n*-type material the figure of merit grows with increase of Seebeck coefficient, and in *p*-type material it first grows and then drops. The average values of thermoelement figure of merit lie within $(2.95 – 2.98)\cdot10^{-3}$ K^{-1}.

It should be noted that we had in our possession the samples prepared by other manufacturers. According to the results of our measurements, their thermoelectric figure of merit did not exceed that obtained on our samples.

In the Harman measurements, contact resistance proves to be included into measured leg resistance. One would think that this automatically solves the problem of account of contact resistance in thermoelectric processes. For temperature-independent thermoelectric parameters such is indeed the case, but actually the situation is more complicated. The point is that temperature field inside the leg is

determined, among other things, by the Joule heat released inside the leg. And it is related to the temperature dependence of material resistivity without regard to contact resistance. Contact resistance becomes apparent only during the processes of heat release on the ends of the leg. Therefore, when measuring by the Harman method, to single out the electric conductivity of material, one should first determine contact resistance.

Contact resistance is most evidently manifested in the leg height dependence of $\Delta T_{\max}$. It is convenient to estimate contact resistance ρ_c by the variation of maximum temperature difference for modules with the different height of legs. If with a change of leg height from l to l' maximum temperature difference varies from $\Delta T_{\max}$ to $\Delta T'_{\max}$, then in the approximation of temperature-independent thermoelectric parameters

$$\rho_c = \frac{\rho}{2}\frac{A}{(\frac{1}{l}-\frac{1}{l'})-\frac{1}{l'}A}, \tag{1}$$

where ρ is material resistivity and

$$A = \frac{\left(\Delta T'_{\max} - \Delta T_{\max}\right)\left(T + \Delta T_{\max}\right)}{\left(T - \Delta T_{\max}\right)\Delta T_{\max}}. \tag{2}$$

From the data for modules of company RMT contact resistance is equal to $2 - 2.5\cdot10^{-6}$ $\Omega\cdot cm^2$. Material electric conductivity σ_m in this case is found from electric conductivity σ_H, measured by the Harman method by means of relation

$$\sigma_m = \frac{\sigma_H}{1-\frac{2\rho_c}{l}\sigma_H}, \tag{3}$$

where l is the height of leg measured by the Harman method. Because of contact resistance, the data on electric conductivity given in Fig. 1 are underrated by 3 – 5 %. The data on the thermoelectric figure of merit are underrated respectively.

Characteristics of thermoelectric modules

Maximum temperature difference on a thermoelement will correspond to its maximum figure of merit Z_{th}. In the approximation of temperature-independent thermoelectric parameters for thermoelement legs having identical section, a condition for matching of couples for reaching maximum Z_{th} is given by the ratio [8]:

$$\sigma_n\kappa_n = \sigma_p\kappa_p. \tag{4}$$

To compare the type of dependences of electric conductivity of *n*- and *p*-type materials, Fig. 5 shows dependences of electric conductivity at 300 and 320 K on the absolute value of Seebeck coefficient at 300 K.

From the above data it is seen that the curves for *n*-type materials are located somewhat higher than the respective curves for *p*-type materials. That is, *n*-type materials have higher specific power than *p*-type materials. Thermal conductivity of *n*-type materials is even somewhat higher than thermal conductivity of *p*-type materials with the identical values of Seebeck coefficient. And in *n*-type materials the relative excess of thermal conductivity proves to be higher than the relative excess of

electric conductivity, as a result of which the thermoelectric figure of merit for *n*-type material proves lower than thermoelectric figure of merit of *p*-type material. But on the whole, to satisfy equation (4), it is necessary that a thermoelement be formed by materials with close absolute values of Seebeck coefficient.

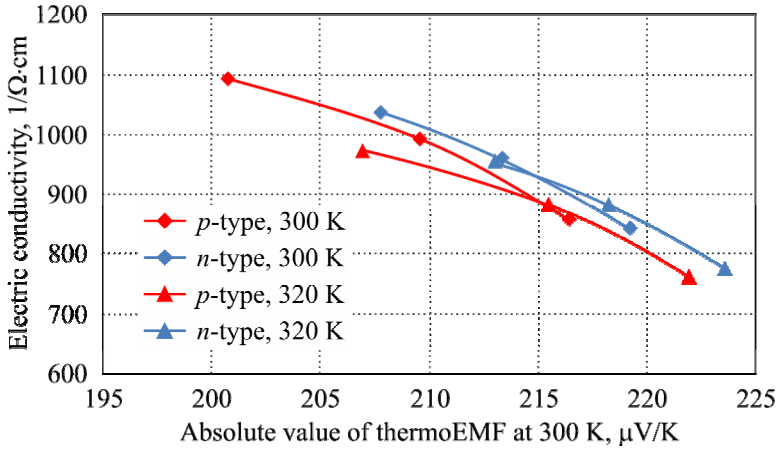

Fig. 5. Dependences of electric conductivity on the absolute value of thermoEMF at 300 K.

However, the temperature dependences of thermoelectric parameters can seriously disturb the validity of (4). Account of temperature dependences can be taken most consecutively by optimal control methods [9]. However, with such a calculation it is difficult to trace a connection to thermal balance equations used with temperature-independent thermoelectric parameters. Therefore, in the calculation we used a model of effective values of thermoelectric parameters [10] that allows keeping the form of thermal balance equation which on the cold end with a zero thermal flow to the cold end of the leg is of the form:

$$\alpha_{c\,eff\,t} T_c I - \frac{1}{2} I^2 R_{c\,eff\,t} - K_{eff\,t} = 0, \tag{5}$$

where T_c is temperature of the cold end of the leg, I is current through the leg, and

$$K_{eff\,t} = \overline{K} = \frac{s}{\int_0^L \frac{dx}{\kappa(T_x)}}, \; t = n, p, \tag{6}$$

where L is leg length, and s is cross-sectional area of t type conductivity leg.

$$R_{c.eff\,t} = \frac{2\overline{K}}{s^2} \int_0^L \rho(T_y) dy \int_y^L \frac{dx}{\kappa(T_x)}, \; t = n, p. \tag{7}$$

$$\alpha_{c.eff\,t} = \alpha(T_C) + \frac{\overline{K}}{sT_c} \int_0^L T_y \frac{d\alpha(T_y)}{dT} \frac{dT}{dy} dy \int_y^L \frac{dx}{\kappa(T_x)}, t = n, p. \tag{8}$$

T_x, T_y is function of temperature distribution along a thermoelement leg. The results of calculation by methods [9] and [10] were compared in [11] and shown to be identical. In order to use formulae (4) – (9), it is necessary to know temperature distribution along the legs. For this purpose, one should first solve thermal conductivity equation, being given by certain initial boundary conditions, and then, using successive approximations method, find at given hot end temperature of leg T_h minimum achievable temperature T_c.

The results of calculation are given in Table 1.

Table 1

Results of calculation of ΔT_{max} for different combinations of n- and p-type couples at the hot end temperature of thermoelement T_h = 300 K

α_p at 300 K / α_n at 300 K	200 μV/K	210 μV/K	216 μV/K
	ΔT_{max}, K		
– 208 μV/K	73.6(72.39)	74.5	74.6
– 213 μV/K	73.7	74.6(74.27)	74.9
– 219 μV/K	73.5	74.6	75.2(74.35)

It is seen that the difference in ΔT_{max} achieves two degrees, whereas, based on the average value of thermoelement efficiency, it should not exceed 0.3 K. Condition (4) for matching of the electrical properties of legs with account of temperature dependences takes on the form:

$$\sigma_{ceff\,n}\kappa_{ceff\,n} = \sigma_{ceff\,p}\kappa_{ceff\,p}, \tag{9}$$

where the respective values of electric conductivity and thermal conductivity are found from (6) and (7). Table 2 lists the calculated values of legs mismatch parameter δ

$$\delta = \frac{\sigma_{ceff\,n}\kappa_{ceff\,n}}{\sigma_{ceff\,p}\kappa_{ceff\,p}} - 1. \tag{10}$$

Table 2

Results of calculation of legs mismatch parameter δ for different combinations of n- and p-type couples

α_p at 300 K / α_n at 300 K	200 μV/K	210 μV/K	216 μV/K
	δ , %		
–208 μV/K	–6.3	7.0	37
–213 μV/K	–16.1	–4.1	22.7
–219 μV/K	–32.6	–23.4	–1.5

From the table it is evident that an ideally matched couple includes materials with α_n = –219 μV/K and α_p = 216 μV/K, yielding the highest value of ΔT_{max} according to Table 1. The diagonal elements of the table are best matched. In so doing, the absolute value of Seebeck coefficient of *n*-type is several units higher than Seebeck coefficient of *p*-type. The data in Table 1 agree with these results. Thus, criterion of proximity of the absolute values of Seebeck coefficient for a couple of thermoelement legs is sufficiently valid and convenient for practical use.

Experimental verification of the compatibility of thermoelement leg couples was done by direct measurement of ΔT_{max} for modules specially assembled of legs with different properties. The measured results are also given in Table 1 in brackets. Comparison of the experimental and calculated data shows sufficiently good agreement of the results. And the calculation correctly reflects the experimentally observed tendency to ΔT_{max} increase with growth of the absolute values of Seebeck coefficient.

Conclusions

The temperature dependences of thermoelectric parameters of extruded thermoelectric materials mass-produced by company RMT (Russia) have been measured by the Harman method. The thermoelectric figure of merit at 300 K was $(3.05 – 3.13)\cdot10^{-3}$ K^{-1} for *p*-type and $(2.83 – 2.87)\cdot10^{-3}$ K^{-1} for *n*-type. Unlike crystalline materials based on bismuth and antimony chalkogenides, the thermoelectric properties of *n*- and *p*-type extruded materials vary notably. Consideration of matching in thermoelement of legs of such materials shows that similarity of absolute Seebeck coefficient values at room temperature for a couple of thermoelement legs is sufficiently good and convenient condition for practical application.

References

1. L.D. Ivanova, Yu.V. Granatkina, and Yu.A. Sidorov, Electrophysical Properties of Antimony Telluride Single Crystals Doped with Selenium and Bismuth, *Inorganic Materials* **1**, 44 – 52 (1999).
2. V.A. Kutasov et al., Anisotropy of Properties of $Bi_2Te_{3-x}Se_x$ Single Crystals, *Physics of the Solid State* **29**(10), 3008 – 3011 (1987).
3. V.N. Abrutin, I.A. Drabkin, and L.B. Ershova, Curl Currents Occurrence in Homogeneous Isotropic Thermoelectric Elements, *Proc. of 5th European Conference on Thermoelectrics* (Odessa, September 10-12, 2007), pp. 163 – 165.
4. T.C. Harman, J.M. Honig, Special Techniques for Measurement of Thermoelectric Properties, *J. Appl. Physics* **29**, 1373 – 1375 (1959).
5. V. Abrutin, I. Drabkin, and V. Osvenski, Corrections Used when Measuring Materials Thermoelectric Properties by Harman Method, *Proc. of 2nd European Conference on Thermoelectrics* (Krakov, September 15-17, 2004).
6. D. Vasilevsky, N. Kukhar, S. Turenne, and R.A. Masur, Hot Extruded $(Bi, Sb)_2(Te, Se)_3$ Alloys for Advanced Thermoelectric Modules, *Proc. of 5th European Conference on Thermoelectrics* (Odessa, September 10-12, 2007), pp. 64 – 67.
7. L.D. Ivanova, L.I. Petrova, and Yu.V. Granatkina, Extruded Materials of Solid Solutions of Bismuth and Antimony Chalcogenides, *Thermoelectrics and Their Applications* (Saint-Petersburg, 2008), pp. 246 – 251.
8. *Thermoelectric Coolers*, Ed. by A.L. Vainer (Moscow: Radio and Sviaz, 1983), 173 p.
9. L.I. Anatychuk, V.A. Semenyuk, *Optimal Control over the Properties of Thermoelectric Materials and Devices* (Chernivtsi: Prut, 1992).
10. I.A. Drabkin, Z.M. Dashevsky, Basic Energy Relations for the Cooling Leg with Regard to Temperature Dependences of Thermoelectric Parameters, *Thermoelectrics and their Applications* (Saint-Petersburg, 2000), pp. 292 – 297.
11. I.A. Drabkin, L.B. Ershova, Comparison of Different Approaches to Optimization of Single-Stage Thermoelectric Modules, *Thermoelectrics and Their Applications* (Saint-Petersburg, 2006), pp. 378 – 390.

Submitted 04.06.2014.